Computers in Biology and Medicine 167 (2023) 107612

Contents lists available at ScienceDirect

Computers in Biology and Medicine

journal homepage: www.elsevier.com/locate/compbiomed

Predicting very early recurrence in intrahepatic cholangiocarcinoma after curative hepatectomy using machine learning radiomics based on CECT: A multi-institutional study

Bo Chen [a,b,1], Yicheng Mao [c,1], Jiacheng Li [a,b,1], Zhengxiao Zhao [d], Qiwen Chen [a,b], Yaoyao Yu [e], Yunjun Yang [e], Yulong Dong [f], Ganglian Lin [a,b], Jiangqiao Yao [a,b], Mengmeng Lu [a,b], Lijun Wu [a], Zhiyuan Bo [a,b,**], Gang Chen [a,b,*], Xiaozai Xie [a,b,***]

[a] Department of Hepatobiliary Surgery, The First Affiliated Hospital of Wenzhou Medical University, Wenzhou, Zhejiang 325035, China
[b] Zhejiang-Germany Interdisciplinary Joint Laboratory of Hepatobiliary-Pancreatic Tumor and Bioengineering, The First Affiliated Hospital of Wenzhou Medical University, Wenzhou, Zhejiang 325035, China
[c] Department of Optometry and Ophthalmology College, Wenzhou Medical University, Wenzhou, Zhejiang 325035, China
[d] Department of Oncology, The First Affiliated Hospital of Zhejiang Chinese Medical University, Hangzhou, Zhejiang 310000, China
[e] Department of Radiology, The First Affiliated Hospital of Wenzhou Medical University, Wenzhou, Zhejiang 325035, China
[f] Department of Oncology, The Eastern Hepatobiliary Surgery Hospital, Naval Medical University, Shanghai 200438, China

ARTICLE INFO

Keywords:
Intrahepatic cholangiocarcinoma
Very early recurrence
Radiomics
Machine learning
Imaging subtype

ABSTRACT

Background: Even after curative resection, the prognosis for patients with intrahepatic cholangiocarcinoma (iCCA) remains disappointing due to the extremely high incidence of postoperative recurrence.
Methods: A total of 280 iCCA patients following curative hepatectomy from three independent institutions were recruited to establish the retrospective multicenter cohort study. The very early recurrence (VER) of iCCA was defined as the appearance of recurrence within 6 months. The 3D tumor region of interest (ROI) derived from contrast-enhanced CT (CECT) was used for radiomics analysis. The independent clinical predictors for VER were histological stage, AJCC stage, and CA199 levels. We implemented K-means clustering algorithm to investigate novel radiomics-based subtypes of iCCA. Six types of machine learning (ML) algorithms were performed for VER prediction, including logistic, random forest (RF), neural network, bayes, support vector machine (SVM), and eXtreme Gradient Boosting (XGBoost). Additionally, six clinical ML (CML) models and six radiomics-clinical ML (RCML) models were developed to predict VER. Predictive performance was internally validated by 10-fold cross-validation in the training cohort, and further evaluated in the external validation cohort.
Results: Approximately 30 % of patients with iCCA experienced VER with extremely discouraging outcome (Hazard ratio (HR) = 5.77, 95 % Confidence Interval (CI) = 3.73–8.93, $P < 0.001$). Two distinct iCCA subtypes based on radiomics features were identified, and subtype 2 harbored a higher proportion of VER (47.62 % Vs 25.53 %) and significant shorter survival time than subtype 1. The average AUC values of the CML and RCML models were 0.744 ± 0.018, and 0.900 ± 0.014 in the training cohort, and 0.769 ± 0.065 and 0.929 ± 0.027 in the external validation cohort, respectively.
Conclusion: Two radiomics-based iCCA subtypes were identified, and six RCML models were developed to predict VER of iCCA, which can be used as valid tools to guide individualized management in clinical practice.

* Corresponding author. Department of Hepatobiliary Surgery, The First Affiliated Hospital of Wenzhou Medical University, Wenzhou, Zhejiang 325035, China.
** Corresponding author. Department of Hepatobiliary Surgery, The First Affiliated Hospital of Wenzhou Medical University, Wenzhou, Zhejiang 325035, China.
*** Corresponding author. Department of Hepatobiliary Surgery, The First Affiliated Hospital of Wenzhou Medical University, Wenzhou, Zhejiang 325035, China.
E-mail addresses: drbozhiyuan@163.com (Z. Bo), chen.gang@wmu.edu.cn (G. Chen), xxiaozai@hotmail.com (X. Xie).
[1] These authors have contributed equally to this work.

https://doi.org/10.1016/j.compbiomed.2023.107612
Received 17 July 2023; Received in revised form 11 October 2023; Accepted 23 October 2023
Available online 31 October 2023

1. Introduction

Intrahepatic cholangiocarcinoma (iCCA), a nearly universally fatal malignancy, represents the second most primary liver malignancy, which has received widespread attention over recent years given the progressive increasing incidence worldwide [1]. The management of iCCA is usually determined by patient- and tumor-specific factors, and therapeutic considerations include surgical resection, transplantation, liver-directed therapies, and systemic therapy [2]. From a curative perspective, major liver resection has been the most appropriate choice, but only a minority of patients (12%–30 %) have resectable disease at the time of diagnosis [3–5]. However, the prognosis of these patients is still unsatisfactory, with a 5-year overall survival (OS) rate of approximately 30 % [6,7] and a median OS of a 30 months [8]. The main reason for this unfavorable postoperative long-term outcome is the extremely high incidence of tumor recurrence, ranging from 50 to 70 % [9,10]. Thus, there is an urgent need to explore novel excellent strategies for postoperative recurrence prediction that can facilitate immediate surveillance and intervention (i.e., systemic chemotherapy) management in high-risk populations.

The etiology of iCCA is complex and difficult to diagnose. Some iCCA patients are not even fully identified before surgery, which may lead to incomplete surgical resection [11]. Additionally, the biological behavior of iCCA is highly aggressive and metastatic, prone to local recurrence or metastasis after radical surgery, especially in patients presented with large tumors, lymph node metastases, and poor nutritional status [12–15]. Previous studies suggested that risk of recurrence following curative resection of iCCA can be influenced by various preoperative clinic-pathologic risk factors, including tumor size, macro and micro vascular invasion, CA199 levels, as well as lymph node metastasis status, and corresponding predictive models have been developed based on these factors [12,16–18]. However, patients with similar clinical characteristics can still exhibit different recurrence patterns, leading to the suboptimal performance of predictive models in previous studies [2]. Radiomics is an emerging interdisciplinary field that integrates medical imaging and computer technology, which enables in-depth analysis of tumor characteristics, including morphology, texture, blood flow, as well as molecular structure and metabolism, through medical image data mining and artificial intelligence [19,20]. By harnessing these imaging biomarkers, radiomics can enhance diagnostic accuracy, prognostication, and treatment response prediction for cancers [21], and its application is well established in liver tumors [22,23]. Our recent study also showed that machine learning radiomics based on preoperative contrast-enhanced CT could accurately predict patient sensitivity to lenvatinib treatment [24]. Compared with classical clinical and pathological factors, radiomics has shown obvious predictive advantages, but studies on recurrence patterns of intrahepatic cholangiocarcinoma are still lacking.

The timing of recurrence following radical hepatectomy can vary markedly among iCCA patients. Previous studies have mostly focused on early recurrence (<12 months), recurrence (12–24 months), and late recurrence (>24months) of iCCA, and found that they have completely different patterns, predictors, and outcomes [9,25]. Notably, Tsilimigras et al. explored the notion of very early recurrence (VER), defined as tumor recurrence within 6 months of hepatectomy, and showed that roughly one-quarter of iCCA patients had VER with extremely poor outcome, which is more common than late recurrence [26]. Therefore, the aim of this study was to apply machine learning approach to investigate the prediction and subtype identification of radiomics in VER of iCCA, based on a multicenter fine-gathered cohort.

2. Methods

2.1. Patient cohorts

From June 1, 2011, to September 1, 2021, a total of 280 consecutive patients with pathologically confirmed iCCA receiving surgical resection were screened in three independent institutions, including The First Affiliated Hospital of Wenzhou Medical University, Eastern Hepatobiliary Surgery Hospital of Naval Medical University and The First Affiliated Hospital of Zhejiang Chinese Medical University. The exclusion criteria were as follows: (1) Without dynamic CECT images within one month prior to surgery; (2) Did not receive curative hepatectomy; (3) Performance status (PS) score >2 or Child-Pugh score >7; (4) Combined with other malignancies; (5) Received other anti-tumor therapies prior to the surgery; (6) Patients died or were lost to follow-up within 6 months after resection without any evidence of recurrence. This study was approved by the institutional ethics review boards and adhered to the Declaration of Helsinki. Since this was a retrospective study, informed consent was not required. This study adhered to the reporting standards outlined in the TRIPOD statement **(**Supplementary Table S1**)**.

2.2. Data collection

Demographic data, including age, gender, and body mass index (BMI, calculated as weight/height^2) were extracted. PS score, Hepatitis B status, liver cirrhosis, Child-Pugh, and laboratory test, including prothrombin, total bilirubin (TBIL), albumin (ALB), alanine aminotransferase (ALT), and aspartate aminotransferase (AST), were used to evaluate patients' activities of daily living and liver function. Tumor characteristics of patients with iCCA were collected, including tumor diameter, tumor number, histological stage, lymph node assessment, perineural invasion, vascular invasion, and AJCC stage (defined following the 8th edition of the American Joint Committee on Cancer staging system) [27]. The latest preoperative blood tumor markers, including alpha-fetoprotein (AFP), carcinoembryonic antigen (CEA), and carbohydrate antigen 199 (CA199) were incorporated. Major hepatectomy was defined as removal of three or more segments.

2.3. Primary outcomes and follow-up surveillance

The VER of iCCA was defined as the appearance of recurrence within 6 months after surgery. All patients with iCCA included into this study received radical hepatectomy. After resection, our multidisciplinary team (MDT) developed a stringent protocol to monitor tumor recurrence in patients, employing serum tumor markers, ultrasonography, CT, and/or magnetic resonance imaging (MRI), and enacted treatment strategies for patients with recurrence. Patients are required to follow up once within the first month after surgery, then once every three months for the first two years, and subsequently once every six months thereafter. Disease recurrence was diagnosed with suspicious radiologic findings or histologically confirmed disease. Overall survival (OS) refers to the interval between the date of surgery and the date of death from any cause, while recurrence-free survival (RFS) refers to the interval between the date of surgery and the date of iCCA recurrence.

2.4. Region segmentation and radiomics analysis

Image contrast-enhanced CT (CECT) with 5-mm-thick sections was used for radiomics analysis. CT acquisition and reconstruction parameters from different institutions are explained in Supplementary Table S2. The contents are as follows: tube voltage, 110–120 kVp; tube current, 130–375 mAs; rotation time, 0.5–0.8 s; image matrix, 512 × 512; pixel spacing, 0.5–0.8 mm; and reconstruction interval, 5 mm. The nonionic contrast agents used were ioversol (Liebel-Flarsheim Canada Inc., Quebec, Canada) and iohexol (Yangtze River Pharmaceutical Group, Taizhou, China). The dosage administered for the nonionic contrast agent was 1.5 mL/kg of body weight, injected intravenously at a rate of 3 mL/s. The arterial phase and portal venous phase CT scans were performed at 25–30 s and 60–75 s post-injection, respectively. Two veteran radiologists with 8 years (Reader 1: YY Y) and 20 years (Reader

2: YJ Y) of experience in liver imaging blinded to clinicopathologic information independently reviewed the CECT images. For arterial and portal venous phases, the 3D tumor region of interest (ROI) image was manually segmented slice by slice using the MRIcroGL software. In the presence of multiple tumors, the lesion with the greatest axial dimensions was preferentially designated for subsequent examination. Moreover, reader 2 contoured the ROI on the 3D tumor images twice within one week. Subsequently, we implemented python package "pyradiomics" (https://pyradiomics.readthedocs.io/en/latest/index.html) [28] to extracted features, including shape-based, first order statistical, Gy level cooccurrence matrix (Glcm), Gy level run length matrix (Glrlm), Gy level size zone matrix (Glszm), Gy level dependence matrix (Gldm), and neighboring gray tone difference matrix (Ngtdm) features. The intra- and inter-observer correlation coefficient analysis was performed to assess the feature stability. The inter-observer agreement analysis was conduct between the extraction of radiomics features by two readers, and intra-observer analysis was implemented using the twice extraction of reader 2 with "irr" R package. Only radiomics features with inter-observer interclass correlation coefficient (ICC) values > 0.75 and intra-observer ICC >0.75 were selected for further research.

The radiomics features contoured by reader 2 was preferentially chosen for the subsequent analysis. Z-score standardization method was performed to normalize these features, then independent samples *t*-test was employed to exclude metrics that showed no significant difference between the groups. Furthermore, we applied the maximum relevance minimum redundancy (mRMR) algorithm to evaluate the importance of features.

2.5. Subtype identification

The identification of molecular subtypes of cancers can facilitate clinical diagnosis and differential diagnosis, guide prognosis assessment and treatment regimen selection, and enable precision medicine and personalized care [29]. Radiomics can provide abundant quantitative data for oncological research and precision management. Consequently, we endeavored to investigate novel molecular subtypes of iCCA through clustering image features, which may correspond to molecular characteristics and pathogenesis of the tumor. The K-means clustering algorithm, a non-supervised learning technique, was utilized to classify the curated metrics. Through K-means clustering, distinct subtypes or clusters of diseases can be determined based on shared features or patterns within the data. This information can provide valuable insights, revealing the heterogeneity of diseases and potentially leading to improvements in diagnosis, treatment selection, and personalized medicine approaches. "NbClust" R package was used to perform K-means clustering and determine the optimal number of clusters [30]. It provides 30 indices which determine the number of clusters in a data set and the number with the most supported indices is considered the optimal number of clusters. Having identified novel radiomics-based iCCA subtypes, we employed chi-square tests to compare percentages among subtypes and investigate the intrinsic associations between CECT and tumor recurrence patterns. Besides, Kaplan-Meier (K-M) survival curves and log-rank tests were utilized to evaluate the correlations between the radiomics subtypes and survival outcomes (including both OS and RFS).

2.6. Machine learning algorithms for VER prediction

Patients with iCCA from three independent institutions were randomly divided into the training and external cohorts with a ratio of 7:3. We utilized an integrated SMOTETomek method combing oversampling and under-sampling to rectify imbalances with "imbalanced-learn" python package in the training cohort. Patients constituting the training set were employed to construct the models and subjected to 10-fold cross validation internally, and patients with iCCA in the external cohort were utilized to examine the proficiency of the resultant models.

The screened radiomic features were ranked in descending order of importance score obtained from the minimum redundancy maximum relevance (mRMR) method. The features were then entered into the logistic regression model one by one. The area under the curve (AUC) was gauged for predicting VER, and the concomitant propensities were examined. We selected the number of features before the turning point and included them in the logistic regression model, thus calculating the radiomics score for subsequent analysis. As for clinicopathologic variables, independent factors were obtained through the univariate and multivariate logistic regression.

First, based on independent clinicopathologic predictors, six types of clinical machine learning (CML) models were developed to predict VER of patients with iCCA in the training cohort, including logistic, random forest (RF), neural network, bayes, support vector machine (SVM), and eXtreme Gradient Boosting (XGBoost). Furthermore, we incorporated radiomics score to construct corresponding six types of radiomics-clinical machine learning (RCML) models to potentiate the prognosticating merit. The 10-cross validation analysis was adopted to assess and compare the above-mentioned models. External validation is imperative when constructing classifiers. The CECT information and clinicopathologic factors were extracted from the external cohort and substituted into the CML and RCML models. The prediction accuracy was verified by the receiver operating characteristic (ROC) curves, calibration curves, and decision curve analysis (DCA). In addition, bootstrapping algorithm with 5000 resamples was applied to evaluated the AUC values with 95 % confident interval (CI) of CML and RCML models.

2.7. Statistical analysis

All statistical analyses were implemented with SPSS 26.0, R software (version 4.0.2), and Python (version 3.9.1). A P-value <0.05 (two tailed) was deemed statistically significant. Numerical variables conforming to normal distribution were expressed as mean $\pm$ standard deviation (SD), and intergroup differences were evaluated using independent samples *t*-test; those not conforming to normal distribution were denoted by median and interquartile range, and intergroup differences were assessed by Wilcoxon signed-rank test. Categorical variables were represented by percentage, and intergroup differences were compared using chi-square test or Fisher's exact test.

3. Results

3.1. Characteristics of iCCA patients with or without VER

The workflow is shown in Fig. 1. A total of 280 iCCA patients following curative hepatectomy from three independent institutions were incorporated into the initial study, and finally 136 patients encountered the stringent inclusion criteria (Table 1). The mean patient age was 63.77 $\pm$ 10.54 years, and mean BMI was 22.27 $\pm$ 3.18 kg/m^2. Sixty-five patients (47.79 %) were female, and 70 patients (51.47 %) had an PS score$\geq$1. Overall, 34 patients (25.00 %) had Hepatitis B infection, and 35 patients (25.74 %) presented with liver cirrhosis. A subset of patients received adjuvant therapy (31 [22.79 %]), 23 patients (16.91 %) had lymphatic metastasis; only a minority of individuals were amenable to laparoscopy. Twenty-two patients (16.18 %) had multiple lesions, and the specific number of lesions for each iCCA patient with multiple tumors are shown in Supplementary Table S3.

Forty-four patients (32.35 %) experienced VER after curative hepatectomy, whereas 92 patients (67.65 %) did not. Fifty-seven patients (41.91 %) had recurrence more than 6 months postoperatively, whereas 35 patients (25.74 %) showed no recurrence during the follow-up period. There were a few significant differences in clinicopathologic variables between VER and non-VER groups. We found iCCA patients with VER tended to have low-undifferentiated histological stage ($P = 0.005$), higher AJCC stage (stage III-IV, $P = 0.001$), lymph node metastasis ($P = 0.026$), and higher preoperative CA199 levels ($P <$

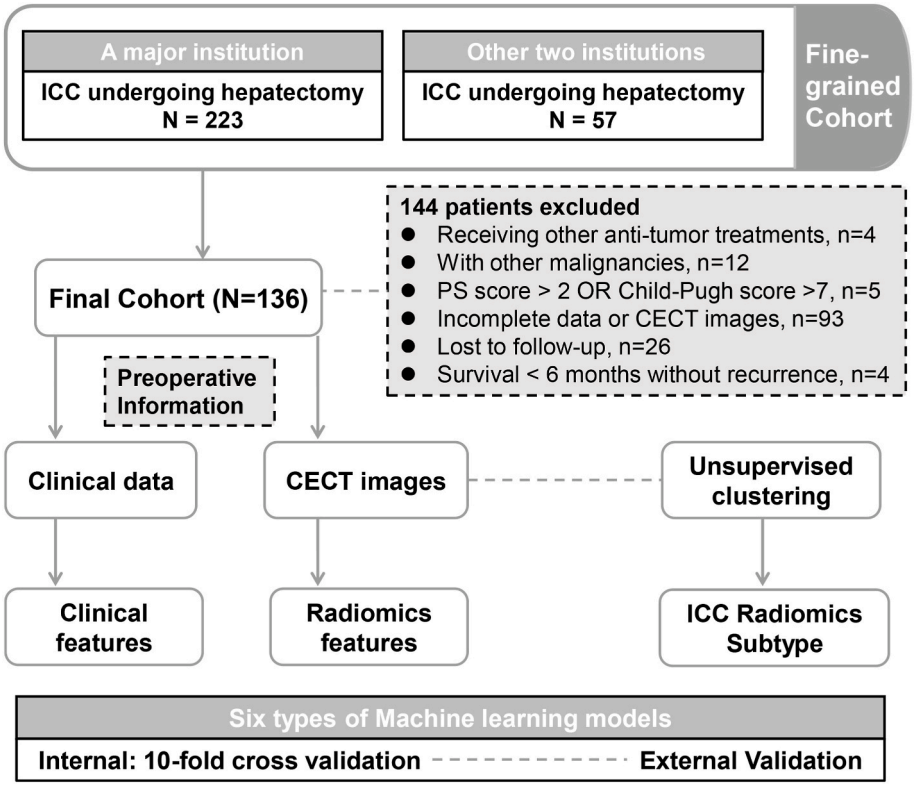

Fig. 1. The workflow of the present study.

0.001). The distribution of major hepatectomy did not differ between the two groups, but a significantly higher proportion of the patients with VER underwent laparoscopy (P = 0.024).

3.2. Prognosis and clinicopathologic predictors of patients with VER

Patients with VER had significantly worse survival than the patients without VER (Hazard ratio [HR] = 5.77, 95%CI = 3.73–8.93, P < 0.001) (Fig. 2). The overall survival rates at 12, 24, and 36 months were 83.5 %, 62.9 %, and 50.4 % for patients without VER respectively, compared to 22.7 %, 6.8 %, and 3.4 % for patients with VER (Table 1). Notably, univariate and multivariable logistic analyses suggested that low-undifferentiated histological stage (Odds ratio [OR] = 3.017, 95%CI = 1.237–7.359, P = 0.015), III-IV AJCC stage (OR = 2.774, 95%CI = 1.217–6.319, P = 0.015), and higher CA199 levels (OR = 1.000, 95%CI = 1.000–1.000, P = 0.013) (Table 2) were independent predictors of VER in patients with iCCA, which were to be utilized for subsequent modeling.

3.3. Identification of novel radiomics-based imaging subtypes in iCCA

The inter- and intra-observer average Hausdorff distances for the segmented ROIs of each patient are shown in Supplementary Table S4. We extracted 214 total radiomics features from each patient: 107 features from the arterial phase and 107 features from the venous phase images, respectively (Supplementary Fig. 1). These include 36 first-order statistical features, 28 shape-based features, 48 GLCM, 32 GLRLM, 32 GLSZM, 28 GLDM, and 10 NGTDM features (Supplementary Table S5). After inter- and intra-reader screening criteria (ICC>0.75) and independent samples *t*-test (P < 0.05), 40 significant features were preliminarily selected.

K-means clustering analysis of the 40 significant features determined that the optimal number of subtypes is 2 (Supplementary Fig. 2). Two distinct imaging iCCA subtypes were identified: subtype 1 (n = 94, 69.12 %) and subtype 2 (n = 42, 30.88 %) (Fig. 3A). We found iCCA patients in the subtype 2 had a higher proportion of VER than subtype 1 (47.62 % Vs 25.53 %) (Fig. 3B–C). Additionally, subtype 2 patients presented significant extremely poor OS (HR = 1.64, 95%CI = 1.03–2.61, P = 0.02) and RFS (HR = 1.80, 95%CI = 1.14–2.86, P = 0.004) than subtype 1 (Fig. 3D–E), which may be associated with distinct pathophysiological mechanisms and biological characteristics.

3.4. Machine learning models based on radiomics features to predict VER

The importance of 40 features ranked by mRMR method was shown in Fig. 4A. The AUC value of the most important feature was 0.682, and by sequentially adding increasing numbers of radiomics features in descending order of importance, the AUC value gradually increased (Fig. 4B). We found that when the number of features reached 35, the AUC value achieved the maximum of 0.916. Adding more features beyond that did not further increase the value. Therefore, we established the radiomics model based on these 35 features.

The clinical variables between the training and external validation sets are listed in Supplementary Table S6, and most variables were randomly distributed. Six clinical machine learning (CML) models were developed based on the three independent predictors with 10-corss validation analysis to predict VER of patients with iCCA. The mean AUC value was 0.744 ± 0.018 (Fig. 5A). Among them, Logistic and SVM demonstrated superior predictive performance, and SVM showed the best performance with an AUC value of 0.770. Subsequently, we built six radiomics-clinical ML (RCML) models (mean AUC of 0.900 ± 0.014) integrating both clinical and radiomics features (Fig. 5B), and the performance was significantly improved compared to the CML models. Notably, the Neural network model achieved the highest AUC value of 0.919.

Table 1
Clinical characteristics between patients with and without very early recurrence within 6 months after curative hepatectomy for intrahepatic cholangiocarcinoma.

Variables	No. (%)			
	Total (N = 136)	VER (N = 44)	Non-VER (N = 92)	P value
Baseline information				
Age, year	63.77 ± 10.54	62.73 ± 9.68	64.27 ± 10.94	0.426
Gender				0.266
Female	65 (47.79 %)	18 (40.90 %)	47 (51.09 %)	
Male	71 (52.21 %)	26 (59.09 %)	45 (48.91 %)	
BMI, kg/m^2	22.27 ± 3.18	22.11 ± 2.65	22.35 ± 3.42	0.685
PS Score				0.812
0	66 (48.53 %)	22 (50.00 %)	44 (47.82 %)	
≥1	70 (51.47 %)	22 (50.00 %)	48 (52.17 %)	
Hepatitis B	34 (25.00 %)	12 (27.27 %)	22 (23.91 %)	0.672
Liver cirrhosis	35 (25.74 %)	11 (25.00 %)	24 (26.09 %)	0.892
Child-Pugh B	14 (10.29 %)	4 (9.09 %)	10 (10.87 %)	0.749
Adjuvant therapy	31 (22.79 %)	10 (22.73 %)	21 (22.83 %)	0.990
Tumor characteristics				
Tumor diameter, cm	5.00 (3.50)	5.00 (3.00)	5.00 (3.00)	0.088
Tumor number (≥2)	22 (16.18 %)	9 (20.45 %)	13 (14.13 %)	0.349
Histological stage				**0.005**
Moderate-High	106 (77.94 %)	28 (63.64 %)	78 (84.78 %)	
Low-Undifferentiated	30 (22.06 %)	16 (36.36 %)	14 (15.22 %)	
AJCC stage				**0.001**
I-II	92 (67.65 %)	21 (47.73 %)	71 (77.17 %)	
III-IV	44 (32.35 %)	23 (52.27 %)	21 (22.83 %)	
Lymphatic metastasis, n	23 (16.91 %)	12 (27.27 %)	11 (11.96 %)	**0.026**
Vascular invasion, n	16 (11.76 %)	8 (18.18 %)	8 (8.70 %)	0.108
Perineural invasion, n	27 (19.85 %)	12 (27.27 %)	15 (16.30 %)	0.134
Surgical margin, R1	9 (6.62 %)	4 (9.09 %)	5 (5.43 %)	0.470
Approach, Laparoscopy	15 (11.03 %)	1 (2.27 %)	14 (15.22 %)	**0.024**
Hepatectomy, major	48 (35.29 %)	18 (40.91 %)	30 (32.61 %)	0.343
Laboratory test				
AFP, ng/ml	3.18 (2.70)	3.32 (3.95)	3.02 (2.47)	0.409
CEA, ug/L	3.00 (8.00)	3.95 (17.63)	2.80 (4.08)	0.145
CA199, U/ml	65.85 (644.8)	270.10 (3889.5)	45.45 (228.23)	**<0.001**
TBIL, umol/L	10.00 (7.00)	9.00 (6.00)	11.00 (6.60)	0.060
ALB, g/L	39.10 (6.70)	38.30 (4.98)	39.75 (7.53)	0.153
ALT, IU/L	24.00 (20.00)	26.50 (26.75)	23.50 (20.00)	0.300
AST, IU/L	27.00 (14.80)	30.00 (27.75)	26.00 (14.00)	0.099
Prothrombin, s	13.50 (1.30)	13.45 (0.80)	13.50 (1.48)	0.860
OS, m, median (95%CI)	19.1 (13.6–24.6)	4.9 (1.9–8.0)	37.6 (24.6–50.7)	<0.001
1-year survival rate (%)	63.8 %	22.7 %	83.5 %	<0.001
2-years survival rate (%)	44.4 %	6.8 %	62.9 %	<0.001
3-years survival rate (%)	35.1 %	3.4 %	50.4 %	<0.001

Abbreviations: VER, very early recurrence; BMI, body mass index; PS, performance status; AFP, alpha-fetoprotein; CEA, carcinoembryonic antigen; CA199, carbohydrate antigen 19-9; TBIL, total bilirubin; ALB, albumin; ALT, glutamic-pyruvic transaminase; AST, glutamic oxaloacetic transaminase; OS, overall survival.

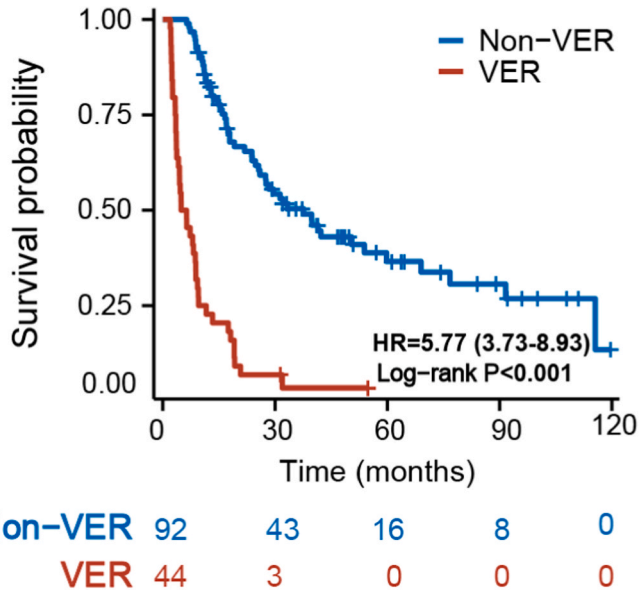

Fig. 2. The Kaplan-Meier (KM) survival curves of patients with iCCA in the VER and Non-VER groups. iCCA, intrahepatic cholangiocarcinoma; VER, very early recurrence.

3.5. External validation of predictive models

Afterwards, the corresponding CECT information and clinical variables were extracted from the patients in the external cohort and substituted to the CML and RCML models. As shown in Fig. 6A and D, the mean AUC values of CML and RCML models were 0.769 ± 0.065 and 0.929 ± 0.027. The random forest model has the best predictive performance in both ways, with the AUC value of 0.891 in the CML model and 0.974 in the RCML model. The calibration curves illustrated excellent consistency between the observed and predicted results of CML and RCML models (Fig. 6B and E). Finally, the DCA curves determined that RCML models serves as a superior tool for clinical VER assessment compared to the CML models (Fig. 6C and F). In addition, the results of bootstrapping algorithm are shown in Supplementary Table S7, which further demonstrate the excellent performance and robustness of the RCML models. To further assess the individual contributions of arterial and venous phase features, we separately incorporated the relevant features to re-establish the clinical-radiomics models. The mean AUCs of the clinical-radiomics model based on arterial phase feature were 0.713 ± 0.045 in the training cohort and 0.801 ± 0.094 in the external validation cohort (Supplementary Fig. 3). The mean AUCs of the clinical-radiomics model based on portal venous phase features were 0.896 ± 0.013 in the training cohort and 0.931 ± 0.035 in the external validation cohort (Supplementary Fig. 4). The clinical-radiomics models constructed solely based on the venous phase performed comparably to the comprehensive models, while the models relying solely on the arterial phase exhibited significantly lower predictive efficacy. In the prediction of postoperative VER in iCCA, features extracted from the venous phase demonstrate greater significance.

To facilitate the convenient utilization of our research findings by surgeons in assessing the risk of postoperative VER in individualized patients with iCCA, we developed a clinical nomogram (Supplementary Fig. 5A) and a radiomics-clinical nomogram (Supplementary Fig. 5B)

Table 2
Bivariate and multivariable logistic regression analyses of factors associated with very early recurrence in patients with intrahepatic cholangiocarcinoma after curative hepatectomy.

Variables	Bivariate logistic analysis		Multivariate logistic analysis	
	OR (95%CI)	P value	OR (95%CI)	P value
Age	0.986 (0.953–1.020)	0.424		
Gender				
Female	Reference			
Male	1.509 (0.729–3.121)	0.267		
BMI	0.977 (0.872–1.094)	0.682		
PS score				
0	Reference			
≥1	0.917 (0.447–1.881)	0.812		
Hepatitis B	1.193 (0.526–2.705)	0.672		
Liver cirrhosis	0.944 (0.413–2.157)	0.892		
Child Pugh score				
A	Reference			
B	0.820 (0.242–2.776)	0.750		
Adjuvant therapy	0.994 (0.422–2.342)	0.990		
Tumor diameter	1.135 (0.979–1.317)	0.094		
Tumor number (≥2)	1.563 (0.611–3.994)	0.351		
Differentiation				
Moderate-High	Reference		Reference	
Low-Undifferentiated	3.184 (1.378–7.354)	**0.007**	3.017 (1.237–7.359)	**0.015**
AJCC stage				
I-II	Reference		Reference	
III-IV	3.703 (1.721–7.967)	**0.001**	2.774 (1.217–6.319)	**0.015**
Lymphatic metastasis	2.761 (1.106–6.893)	**0.030**		
Vascular invasion	2.333 (0.813–6.701)	0.115		
Perineural invasion	1.925 (0.811–4.566)	0.137		
Surgical margin, R1	1.740 (0.443–6.827)	0.427		
Laparoscopy method	0.130 (0.016–1.019)	0.052		
Hepatectomy, Major	1.431 (0.681–3.006)	0.344		
AFP	1.002 (0.999–1.005)	0.301		
CEA	0.999 (0.993–1.004)	0.648		
CA199	1.000 (1.000–1.000)	**0.003**	1.000 (1.000–1.000)	**0.013**
TBIL	0.999 (0.989–1.010)	0.884		
ALB	0.949 (0.881–1.023)	0.172		
ALT	1.001 (0.995–1.006)	0.885		
AST	1.000 (0.993–1.006)	0.890		
Prothrombin	0.921 (0.661–1.284)	0.628		

Abbreviations: BMI, Body mass index; PS, Performance status; HBV, Hepatitis B virus; AFP, Alpha fetoprotein; CEA, carcinoembryonic; Antigen; CA, carbohydrate antigen; TBIL, Total bilirubin; ALB, Albumin; ALT, Alanine aminotransferase; AST, Aspartate aminotransferase; CONUT, Controlling nutritional status; PNI, Prognostic nutritional index; ALBI, Albumin-bilirubin.

that can serve as clinical practical tools.

4. Discussion

Despite effective surgical resection, iCCA still exhibits an extremely high recurrence rate postoperatively, which is attributed to its highly invasive and heterogeneous nature [31]. Previous studies commonly defined early recurrence as recurrence within 1 year or 2 years after surgery and investigated clinical predictors and outcomes [32–34]. However, a considerable proportion of patients with iCCA have been found to relapse much earlier, within the first several months after resection, and they have an extremely poor prognosis but are often overlooked [25,26]. The present study aimed to investigate factors associated with VER (≤6 months) and develop predictive models based on clinical and radiomics features. We found that 32.35 % of patients experienced VER with 1-year survival rate of only 22.7 %. This incidence was higher than the 22.3 % reported in a previous international multicenter cohort study [26]. Preoperative prediction of VER after surgery may help tailor adjuvant treatment strategies, postoperative surveillance, and management. Here, this is the first study to apply ML radiomics using CECT to explore the relationship between imaging subtype and recurrence pattern, and the clinical utility of ML radiomics in predicting VER.

The latest advances in radiomics provide a robust methodology to extract radiological features beyond human visual perception, with the potential to assess tumor biological characteristics, therapeutic response, and oncologic outcomes [35]. The appropriate combination of radiomic features and clinical factors may improve the accuracy of complex clinical decision making [21,36]. Xu et al. constructed a computational approach integrating large-scale clinical and radiomic features on the basis of CECT to predict microvascular invasion and outcomes in patients with hepatocellular carcinoma (HCC), yielding AUCs of 0.909 and 0.889 in the training set and test set, respectively [23]. Chen et al. developed a clinical-radiomics model for preoperatively selecting patients with intermediate-stage HCC who may objectively respond to initial transarterial chemoembolization (TACE) [37]. Employing a multi-institutional cohort, Ji et al. accomplished a radiogenomic study and inferred that CT imaging features can precisely prognosticate the macrotrabecular-massive subcategory in patients with HCC, which are linked to aberrant humoral immunity encompassing B lymphocyte infiltration and immunoglobulin biosynthesis [22]. For liver malignancies, w/o contrast CT primarily serves to roughly determine the tumor's location, while the extent and internal structural features of the tumor are better visualized during the arterial and venous phases of contrast-enhanced CT. Hence, similar to previous studies [22,23,38], we selected only these two phases for analysis. We performed the K-means clustering algorithm to explore potential radiomics-based iCCA imaging subtypes to stratify patients with distant recurrence patterns and clinical outcomes. We discerned that iCCA patients classified into the subtype 2 harbored a higher VER fraction (47.62 % Vs 25.53 %) and significant shorter survival time than subtype 1. This may be associated with the activation of more carcinogenic signaling pathways and immunosuppressive tumor microenvironment in iCCA patients with Subtype 2. Subsequent correlation analysis of tumor genomic, transcriptomic and other molecular biological data is needed to explore the molecular mechanisms behind the imaging features [39]. This classification strategy may assist clinical judgment of iCCA recurrence patterns, achieve preoperative non-invasive preliminary diagnosis, and provide references for clinicians to select the optimal treatment regimen.

The current study developed valuable machine learning models based on clinical and radiomics features to predict VER following curative hepatectomy for patients with iCCA. A single most significant radiomics feature alone suffices to assess VER with the AUC value of 0.682, and an integrated radiomics score of 35 features is proficient at prognosticating VER with the AUC value of 0.916. This may be attributable to radiomic features possessing the potential to further delineate

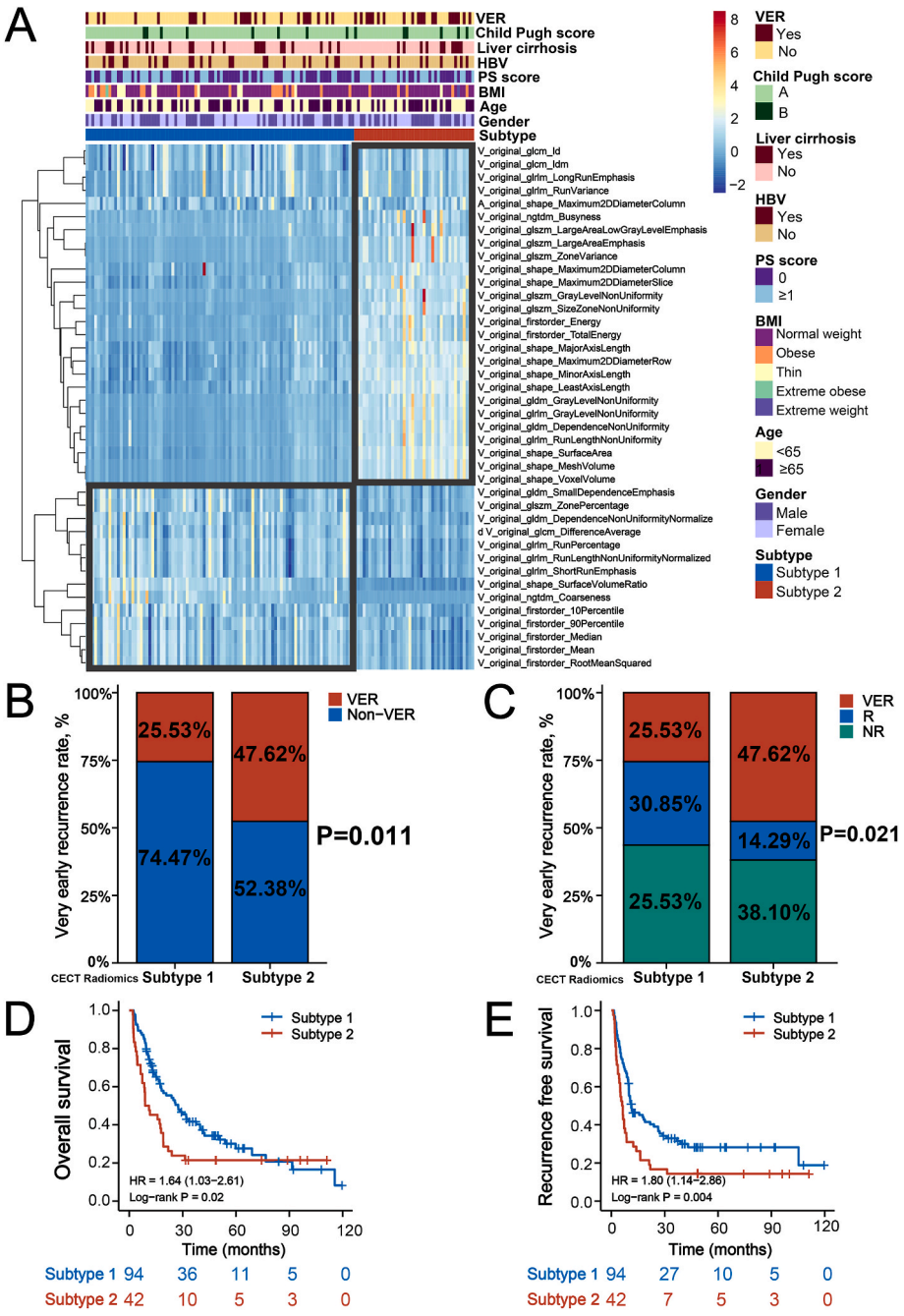

Fig. 3. Identification of two radiomics-related iCCA subtypes. The heatmap of 40 significant radiomics features between the two subtypes (A). Comparison of the compositional difference of recurrence patterns between the two subtypes (B–C). The KM survival curves of overall survival (D) and recurrence-free survival (E) in patients with iCCA between the two subtypes. iCCA, intrahepatic cholangiocarcinoma; VER, very early recurrence; NR, non-recurrence.

the spatial heterogeneity and intrinsic biological characteristics of tumors at multiple scales [40–42]. In addition, some clinical factors were found to be associated with VER, including histological stage, AJCC stage, and CA199, which were in accordance with previous studies. Poor differentiation has been correlated with iCCA recurrence and abbreviated survival in previous studies [8,43]. Augmented neoplastic cellular dysplasia and constituent number are anticipated to endow intensified encroachment predisposition and dissemination possibility in the tumor [44,45]. More advanced tumor stage signifies deeper neoplastic cell invasion into perihepatic tissues and vasculature, which may harbor macroscopically and adjunctively undetectable remnants. Despite radical hepatic resection, higher staged iCCA are prone to eliciting de novo oncogenic mutations. Prolonged progression may activate additional carcinogenesis-related cellular signaling pathways associated with proliferation, angiogenesis and cellular dissemination [46–48]. Similarly, as a vital serum biomarker for gastrointestinal tumor, CA199 could monitor tumor burden. Patients with iCCA harboring elevated presurgical CA199 expression were prone to postoperative recurrence [26]. Compared with these clinical factors, the radiomics score showed stronger predictive accuracy. Radiomic features extracted from CECT such as tumor size, shape irregularity and ill-defined margins can be utilized to assess tumor invasiveness. Radiologic phenotypes are also capable of delineating tumor parenchyma and extracellular matrix, and distinct oncologic imaging modalities can reveal various components within the tumor immune microenvironment [49,50]. The average AUC value of six RCML models established by adding radiomics score was

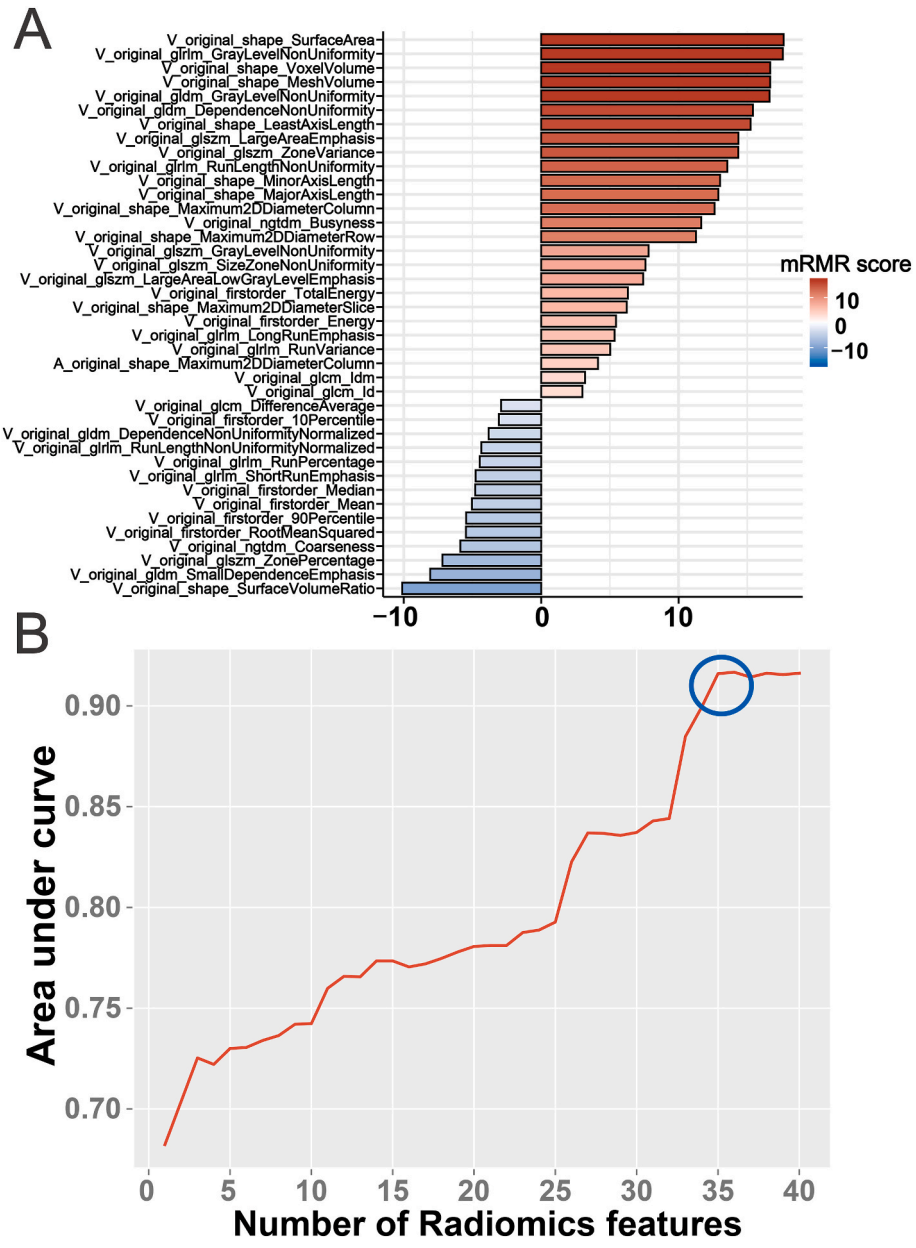

Fig. 4. The importance score of 40 significant radiomics features based on the mRMR algorithm (A). The features were input into the logistic regression model one by one in order of importance, and the AUC value was implemented to evaluate the accuracy of VER prediction (B). mRMR, minimum redundancy maximum relevance; AUC, area under the curve; VER, very early recurrence.

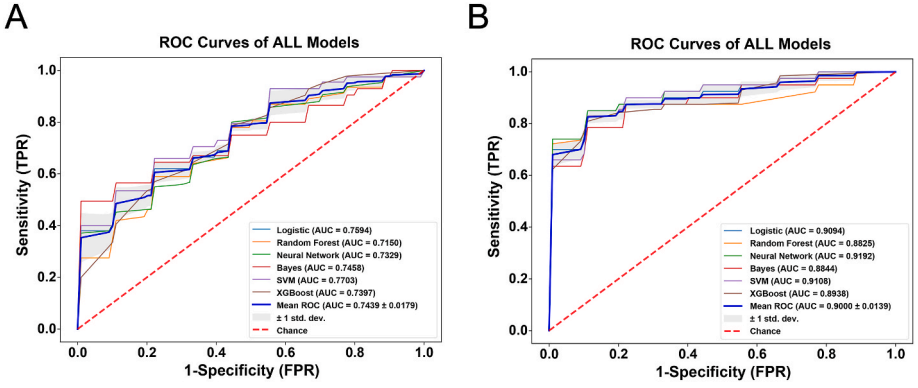

Fig. 5. The average AUC value from 10-fold cross-validation of six clinical machine learning models (A) and six radiomics-clinical machine learning models (B) in the training cohort. AUC, area under the curve.

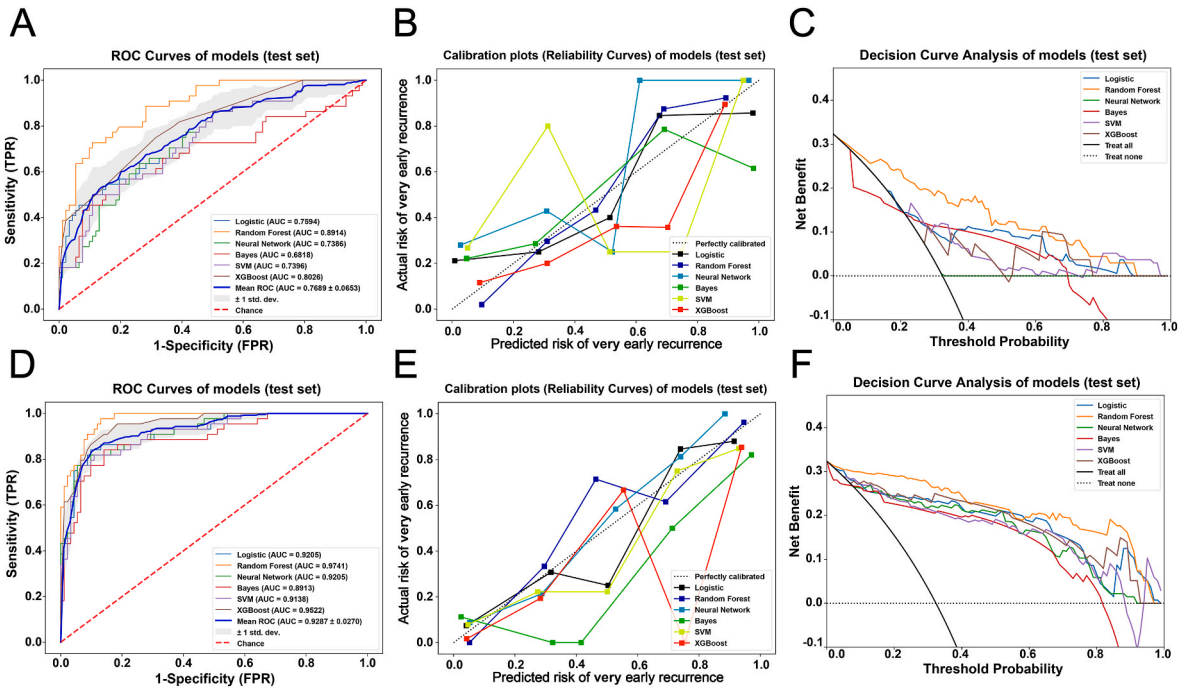

Fig. 6. External validation of clinical and radiomics-clinical machine learning models. The ROC curve analysis (A), calibration curve (B), and decision curve analysis (C) of the six clinical machine learning models. The ROC curve analysis (D), calibration curve (E), and decision curve analysis (F) of the six radiomics-clinical machine learning models. ROC, receiver operating characteristic.

0.900 in the training set and 0.929 in the validation set, which suggested that these models may serve as a powerful predictive tool in future clinical practice.

We applied a combination of self-extracted radiomics features and machine learning algorithms to evaluate the postoperative VER of iCCA. Machine learning (ML) has more flexible requirements for data processing, and relevant features can be selected for learning after artificially extracting data for sorting and labeling. In this study, the widely recognized "Pyradiomics" python package [23,28], known for its high credibility in the field, was utilized to extract conventional features, then screened and modeled by ML algorithms, so it has strong interpretability and expansibility. However, deep learning radiomics (DLR), which is better suited for utilizing raw data and automatically extracting features, possesses a complex internal structure that enables accurate results but compromises interpretability [51,52]. Radiomic analysis involves the automated extraction of clinically relevant information and potential biological meanings from radiologic images [53]. Elucidating the underlying significance of features may provide new clues regarding the biological drivers of patient outcomes. In this study, the radiomics features closely associated with VER were mostly related to tumor size, 3D shape, texture, and voxel intensity. On the one hand, these features (e.g., Shape_SurfaceArea, VoxelVolume, LeastAxisLength, etc.) offered a more comprehensive three-dimensional representation than the simple tumor size value, which was consistent with previous findings that larger tumors are associated with higher rates of postoperative recurrence. On the other hand, texture and voxel intensity-related features (e.g., glrlm_GrayLevelNonUniformity, gldm_DependenceNonUniformity, glszm_LargeAreaEmphasis, etc.) primarily reflected the heterogeneity of the tumor, with greater values implying greater complexity of the tumor microenvironment (e.g., expression of key oncogenes, immunosuppressive status, and metabolic pattern). A study by Sun et al. identified four types of prognostic radiomics phenotypes based on similar features as in this study and found that they exhibit markedly different immune, proliferative, treatment responsiveness, and cellular function pathway expression profiles [54]. Udayakumar et al. found that tumor features derived from MRI are associated with angiogenesis and inflammation and differed across tumors, which may indicate the effectiveness of anti-angiogenic drugs and immunotherapy [55]. However, due to the lack of genomic and immunohistochemical data, the biological significance of the imaging features associated with VER in this study remains unclear. These features may reflect the biological structure of the tumor and its sensitivity to the tumor microenvironment, serving as a biomarker for more invasive biological behavior in ICC. In future studies, we will conduct transcriptome sequencing analysis on the corresponding samples to further explore the biological significance of the imaging features.

To some extent, our findings are important to predict prognosis and optimize individual management in clinical practice. In the present study, roughly 30 % of patients with iCCA experienced VER with extremely discouraging outcomes. Preoperative identification of patients at high risk of recurrence and provision of aggressive postoperative interventions may improve patient outcomes. Some interventional measures may provide some benefit to improve prognosis. Including adjuvant chemotherapy, local radiotherapy, targeted therapy, immunotherapy, and lifestyle interventions [56,57]. Postoperative adjuvant chemotherapy may reduce the risk of recurrence by eliminating residual disease, but there is still a controversy about the application value of adjuvant chemotherapy [58]. Capecitabine adjuvant chemotherapy has now been adopted as a standard treatment by ASCO [59], and additional clinical trials are ongoing. Additionally, for iCCA patients stratified as high risk before surgery, close follow-up can be utilized for early detection and excision of new lesions. Genetic sequencing can also be selectively performed in high-risk patients to direct targeted therapies (such as FGFR inhibitors, IDH1/2 inhibitors, etc.) towards mutated individuals [60,61]. In this study, we successfully built several radiomics-based predictive models, which can provide significant references to assess the probability of VER. In addition, we identified two radiomics-based imaging subtypes to initially stratify patients into different recurrence patterns. Through our machine learning algorithms, accurate risk stratification and rigorous patient selection for additional treatments can be achieved. This is clinically important for optimizing treatment strategies and guiding clinical

decision-making.

5. Conclusion

Two radiomics-based iCCA subtypes were identified, and six RCML models were developed to predict VER of iCCA, which can be used as valid tools to guide individualized management in clinical practice.

Ethics approval and consent to participate

This study was approved by the institutional ethics review boards and adhered to the Declaration of Helsinki. Our institutional ethics review boards waived the need for informed consent from patients.

Author contributions

BC, XZX, GC, and ZYB were responsible for conception and design. JCL, ZXZ QWC, YLD, and LJW performed the literature search. YJY, and YYY performed region segmentation of CECT. BC, YCM, and ZYB generated the figures and Tables. BC, YCM and GLL analyzed the data. BC, YCM, and JQY wrote the manuscript, and ZYB critically reviewed the manuscript. XZX and GC supervised the research. All authors have read and approved the manuscript.

Consent for publication

Not applicable.

Data accessibility

The datasets and codes generated and analyzed in the current study are available from the corresponding authors upon reasonable request.

Declaration of competing interest

The authors declare that they have no competing interests.

Acknowledgements

This work was supported by National Natural Science Foundation of China (Grant numbers: 82072685) and Science and Technology Innovation Activity Program for College Students in Zhejiang Province (Grant numbers: 2023R413059).

Appendix B. Supplementary data

Supplementary data to this article can be found online at https://doi.org/10.1016/j.compbiomed.2023.107612.

List of abbreviations

iCCA	Intrahepatic cholangiocarcinoma
ML	Machine learning
VER	Very early recurrence
NR	Non-recurrence
mRMR	Minimum redundancy maximum relevance
AUC	Area under the curve
ROC	Receiver operating characteristic
AUC	Area under the curve
CECT	Contrast-enhanced CT
CML	Clinical machine learning
RCML	Radiomics-clinical machine learning
PS	Performance status
OS	Overall survival
RFS	Recurrence-free survival
TBIL	Total bilirubin
ALB	Albumin
ALT	Alanine aminotransferase
AST	Aspartate aminotransferase
CEA	Carcinoembryonic antigen
AFP	Alpha-fetoprotein
CA199	Carbohydrate antigen 199
MDT	Multidisciplinary team
CSCO	Chinese Society of Clinical Oncology
RF	Random forest
SVM	Support vector machine
XGBoost	eXtreme Gradient Boosting

References

[1] A. Sirica, G. Gores, J. Groopman, F. Selaru, M. Strazzabosco, X. Wei Wang, A. Zhu, Intrahepatic cholangiocarcinoma: continuing challenges and translational advances, Hepatology 69 (4) (2019) 1803–1815.
[2] D. Moris, M. Palta, C. Kim, P. Allen, M. Morse, M. Lidsky, Advances in the treatment of intrahepatic cholangiocarcinoma: an overview of the current and future therapeutic landscape for clinicians, CA A Cancer J. Clin. 73 (2) (2023) 198–222.
[3] A. Nakeeb, K. Tran, M. Black, B. Erickson, P. Ritch, E. Quebbeman, S. Wilson, M. Demeure, W. Rilling, K. Dua, et al., Improved survival in resected biliary malignancies, Surgery 132 (4) (2002) 555–563, discission 563-554.
[4] Y. Wada, M. Shimada, K. Yamamura, T. Toshima, J. Banwait, Y. Morine, T. Ikemoto, Y. Saito, H. Baba, M. Mori, et al., A transcriptomic signature for risk-stratification and recurrence prediction in intrahepatic cholangiocarcinoma, Hepatology 74 (3) (2021) 1371–1383.
[5] M. de Jong, H. Nathan, G. Sotiropoulos, A. Paul, S. Alexandrescu, H. Marques, C. Pulitano, E. Barroso, B. Clary, L. Aldrighetti, et al., Intrahepatic cholangiocarcinoma: an international multi-institutional analysis of prognostic factors and lymph node assessment, J. Clin. Oncol. : Off. J. Am. Soc. Clin. Oncol. 29 (23) (2011) 3140–3145.
[6] N. Amini, A. Ejaz, G. Spolverato, Y. Kim, J. Herman, T. Pawlik, Temporal trends in liver-directed therapy of patients with intrahepatic cholangiocarcinoma in the United States: a population-based analysis, J. Surg. Oncol. 110 (2) (2014) 163–170.
[7] R. El-Diwany, T. Pawlik, A. Ejaz, Intrahepatic cholangiocarcinoma, Surg. Oncol. Clin. 28 (4) (2019) 587–599.
[8] M. Mavros, K. Economopoulos, V. Alexiou, T. Pawlik, Treatment and prognosis for patients with intrahepatic cholangiocarcinoma: systematic review and meta-analysis, JAMA Surg. 149 (6) (2014) 565–574.
[9] A. Doussot, M. Gonen, J. Wiggers, B. Groot-Koerkamp, R. DeMatteo, D. Fuks, P. Allen, O. Farges, T. Kingham, J. Regimbeau, et al., Recurrence patterns and disease-free survival after resection of intrahepatic cholangiocarcinoma: preoperative and postoperative prognostic models, J. Am. Coll. Surg. 223 (3) (2016) 493–505.e492.
[10] G. Spolverato, Y. Kim, S. Alexandrescu, H. Marques, J. Lamelas, L. Aldrighetti, T. Clark Gamblin, S. Maithel, C. Pulitano, T. Bauer, et al., Management and outcomes of patients with recurrent intrahepatic cholangiocarcinoma following previous curative-intent surgical resection, Ann. Surg Oncol. 23 (1) (2016) 235–243.
[11] S. Kubo, H. Shinkawa, Y. Asaoka, T. Ioka, H. Igaki, N. Izumi, T. Itoi, M. Unno, M. Ohtsuka, T. Okusaka, et al., Liver cancer study group of Japan clinical practice guidelines for intrahepatic cholangiocarcinoma, Liver Cancer 11 (4) (2022) 290–314.
[12] H. Lang, J. Baumgart, S. Heinrich, T. Huber, L. Heuft, R. Margies, J. Mittler, F. Hahn, T. Gerber, F. Foerster, et al., Liver resection for intrahepatic cholangiocarcinoma-single-center experience with 286 patients undergoing surgical exploration over a thirteen year period, J. Clin. Med. 10 (16) (2021).
[13] C. Sposito, F. Ratti, A. Cucchetti, F. Ardito, A. Ruzzenente, S. Di Sandro, M. Maspero, G. Ercolani, F. Di Benedetto, A. Guglielmi, et al., Survival benefit of adequate lymphadenectomy in patients undergoing liver resection for clinically node-negative intrahepatic cholangiocarcinoma, J. Hepatol. 78 (2) (2023) 356–363.
[14] X. Zhang, F. Xue, D. Dong, M. Weiss, I. Popescu, H. Marques, L. Aldrighetti, S. Maithel, C. Pulitano, T. Bauer, et al., Number and station of lymph node metastasis after curative-intent resection of intrahepatic cholangiocarcinoma impact prognosis, Ann. Surg. 274 (6) (2021) e1187–e1195.
[15] J. Zhu, D. Wang, C. Liu, R. Huang, F. Gao, X. Feng, T. Lan, H. Li, H. Wu, Development and validation of a new prognostic immune-inflammatory-nutritional score for predicting outcomes after curative resection for intrahepatic cholangiocarcinoma: a multicenter study, Front. Immunol. 14 (2023), 1165510.
[16] K. Xing, L. Lu, X. Huang, C. He, Y. Song, R. Guo, S. Li, A novel prognostic nomogram for patients with recurrence of intrahepatic cholangiocarcinoma after initial surgery, Front. Oncol. 10 (2020) 434.
[17] Q. Li, J. Zhang, C. Chen, T. Song, Y. Qiu, X. Mao, H. Wu, Y. He, Z. Cheng, W. Zhai, et al., A nomogram model to predict early recurrence of patients with intrahepatic cholangiocarcinoma for adjuvant chemotherapy guidance: a multi-institutional analysis, Front. Oncol. 12 (2022), 896764.
[18] I. Endo, M. Gonen, A. Yopp, K. Dalal, Q. Zhou, D. Klimstra, M. D'Angelica, R. DeMatteo, Y. Fong, L. Schwartz, et al., Intrahepatic cholangiocarcinoma: rising

frequency, improved survival, and determinants of outcome after resection, Ann. Surg. 248 (1) (2008) 84–96.
[19] P. Lambin, E. Rios-Velazquez, R. Leijenaar, S. Carvalho, R. van Stiphout, P. Granton, C. Zegers, R. Gillies, R. Boellard, A. Dekker, et al., Radiomics: extracting more information from medical images using advanced feature analysis, European journal of cancer (Oxford, England : 1990) 48 (4) (2012) 441–446.
[20] P. Lambin, R. Leijenaar, T. Deist, J. Peerlings, E. de Jong, J. van Timmeren, S. Sanduleanu, R. Larue, A. Even, A. Jochems, et al., Radiomics: the bridge between medical imaging and personalized medicine, Nat. Rev. Clin. Oncol. 14 (12) (2017) 749–762.
[21] K. Bera, N. Braman, A. Gupta, V. Velcheti, A. Madabhushi, Predicting cancer outcomes with radiomics and artificial intelligence in radiology, Nat. Rev. Clin. Oncol. 19 (2) (2022) 132–146.
[22] Z. Feng, H. Li, Q. Liu, J. Duan, W. Zhou, X. Yu, Q. Chen, Z. Liu, W. Wang, P. Rong, CT radiomics to predict macrotrabecular-massive subtype and immune status in hepatocellular carcinoma, Radiology 307 (1) (2023), e221291.
[23] X. Xu, H. Zhang, Q. Liu, S. Sun, J. Zhang, F. Zhu, G. Yang, X. Yan, Y. Zhang, X. Liu, Radiomic analysis of contrast-enhanced CT predicts microvascular invasion and outcome in hepatocellular carcinoma, J. Hepatol. 70 (6) (2019) 1133–1144.
[24] Z. Bo, B. Chen, Z. Zhao, Q. He, Y. Mao, Y. Yang, F. Yao, Y. Yang, Z. Chen, J. Yang, et al., Prediction of response to lenvatinib monotherapy for unresectable hepatocellular carcinoma by machine learning radiomics: a multicenter cohort study, Clin. Cancer Res. : Off. J. Am. Assoc. Cancer Res. 29 (9) (2023) 1730–1740.
[25] X.F. Zhang, E.W. Beal, F. Bagante, J. Chakedis, M. Weiss, I. Popescu, H.P. Marques, L. Aldrighetti, S.K. Maithel, C. Pulitano, et al., Early versus late recurrence of intrahepatic cholangiocarcinoma after resection with curative intent, Br. J. Surg. 105 (7) (2018) 848–856.
[26] D.I. Tsilimigras, K. Sahara, L. Wu, D. Moris, F. Bagante, A. Guglielmi, L. Aldrighetti, M. Weiss, T.W. Bauer, S. Alexandrescu, et al., Very early recurrence after liver resection for intrahepatic cholangiocarcinoma: considering alternative treatment approaches, JAMA Surgery 155 (9) (2020) 823–831.
[27] M.B. Amin, S.B. Edge, F.L. Greene, D.R. Byrd, R.K. Brookland, M.K. Washington, J. E. Gershenwald, C.C. Compton, K.R. Hess, D.C. Sullivan, in: AJCC Cancer Staging Manual, vol. 1024, Springer, 2017.
[28] J. van Griethuysen, A. Fedorov, C. Parmar, A. Hosny, N. Aucoin, V. Narayan, R. Beets-Tan, J. Fillion-Robin, S. Pieper, H. Aerts, Computational radiomics system to decode the radiographic phenotype, Cancer Res. 77 (21) (2017) e104–e107.
[29] Comprehensive molecular profiling of lung adenocarcinoma, Nature 511 (7511) (2014) 543–550.
[30] M. Charrad, N. Ghazzali, V. Boiteau, A. Niknafs, NbClust: an R package for determining the relevant number of clusters in a data set, J. Stat. Software 61 (6) (2014) 1–36.
[31] V. Mazzaferro, A. Gorgen, S. Roayaie, M. Droz Dit Busset, G. Sapisochin, Liver resection and transplantation for intrahepatic cholangiocarcinoma, J. Hepatol. 72 (2) (2020) 364–377.
[32] A. Nassar, S. Tzedakis, R. Sindayigaya, C. Hobeika, U. Marchese, J. Veziant, T. Codjia, A. Beaufrère, A. Dhote, M. Strigalev, et al., Factors of early recurrence after resection for intrahepatic cholangiocarcinoma, World J. Surg. 46 (10) (2022) 2459–2467.
[33] T. Wakiya, K. Ishido, N. Kimura, H. Nagase, T. Kanda, S. Ichiyama, K. Soma, M. Matsuzaka, Y. Sasaki, S. Kubota, et al., CT-based deep learning enables early postoperative recurrence prediction for intrahepatic cholangiocarcinoma, Sci. Rep. 12 (1) (2022) 8428.
[34] L. Xu, Y. Wan, C. Luo, J. Yang, P. Yang, F. Chen, J. Wang, T. Niu, Integrating intratumoral and peritumoral features to predict tumor recurrence in intrahepatic cholangiocarcinoma, Phys. Med. Biol. 66 (12) (2021).
[35] Z. Liu, S. Wang, D. Dong, J. Wei, C. Fang, X. Zhou, K. Sun, L. Li, B. Li, M. Wang, et al., The applications of radiomics in precision diagnosis and treatment of Oncology: opportunities and challenges, Theranostics 9 (5) (2019) 1303–1322.
[36] X. Yin, H. Liao, H. Yun, N. Lin, S. Li, Y. Xiang, X. Ma, Artificial intelligence-based prediction of clinical outcome in immunotherapy and targeted therapy of lung cancer, Semin. Cancer Biol. 86 (Pt 2) (2022) 146–159.
[37] M. Chen, J. Cao, J. Hu, W. Topatana, S. Li, S. Juengpanich, J. Lin, C. Tong, J. Shen, B. Zhang, et al., Clinical-radiomic analysis for pretreatment prediction of objective response to first transarterial chemoembolization in hepatocellular carcinoma, Liver Cancer 10 (1) (2021) 38–51.
[38] H.J. Park, B. Park, S.Y. Park, S.H. Choi, H. Rhee, J.H. Park, E.-S. Cho, S.-K. Yeom, S. Park, M.-S. Park, et al., Preoperative prediction of postsurgical outcomes in mass-forming intrahepatic cholangiocarcinoma based on clinical, radiologic, and radiomics features, Eur. Radiol. 31 (11) (2021) 8638–8648.
[39] K. Pinker, J. Chin, A.N. Melsaether, E.A. Morris, L. Moy, Precision medicine and radiogenomics in breast cancer: new approaches toward diagnosis and treatment, Radiology 287 (3) (2018) 732–747.
[40] Y.-T. Peng, C.-Y. Zhou, P. Lin, D.-Y. Wen, X.-D. Wang, X.-Z. Zhong, D.-H. Pan, Q. Que, X. Li, L. Chen, et al., Preoperative ultrasound radiomics signatures for noninvasive evaluation of biological characteristics of intrahepatic cholangiocarcinoma, Acad. Radiol. 27 (6) (2020) 785–797.
[41] N. Shen, W. Lv, S. Li, D. Liu, Y. Xie, J. Zhang, J. Zhang, J. Jiang, R. Jiang, W. Zhu, Noninvasive evaluation of the notch signaling pathway via radiomic signatures based on multiparametric MRI in association with biological functions of patients with glioma: a multi-institutional study, J. Magn. Reson. Imag. 57 (3) (2023) 884–896.
[42] X. Meng, W. Xia, P. Xie, R. Zhang, W. Li, M. Wang, F. Xiong, Y. Liu, X. Fan, Y. Xie, et al., Preoperative radiomic signature based on multiparametric magnetic resonance imaging for noninvasive evaluation of biological characteristics in rectal cancer, Eur. Radiol. 29 (6) (2019) 3200–3209.
[43] X.-F. Zhang, J. Chakedis, F. Bagante, E.W. Beal, Y. Lv, M. Weiss, I. Popescu, H. P. Marques, L. Aldrighetti, S.K. Maithel, et al., Implications of intrahepatic cholangiocarcinoma etiology on recurrence and prognosis after curative-intent resection: a multi-institutional study, World J. Surg. 42 (3) (2018) 849–857.
[44] Y. Shimada, H. Saji, K. Yoshida, M. Kakihana, H. Honda, M. Nomura, J. Usuda, N. Kajiwara, T. Ohira, N. Ikeda, Pathological vascular invasion and tumor differentiation predict cancer recurrence in stage IA non-small-cell lung cancer after complete surgical resection, J. Thorac. Oncol. 7 (8) (2012) 1263–1270.
[45] S. Vijgen, B. Terris, L. Rubbia-Brandt, Pathology of intrahepatic cholangiocarcinoma, Hepatobiliary Surg. Nutr. 6 (1) (2017) 22–34.
[46] D. Sia, Y. Hoshida, A. Villanueva, S. Roayaie, J. Ferrer, B. Tabak, J. Peix, M. Sole, V. Tovar, C. Alsinet, et al., Integrative molecular analysis of intrahepatic cholangiocarcinoma reveals 2 classes that have different outcomes, Gastroenterology 144 (4) (2013) 829–840.
[47] T. Patel, New insights into the molecular pathogenesis of intrahepatic cholangiocarcinoma, J. Gastroenterol. 49 (2) (2014) 165–172.
[48] M. Wei, L. Lü, P. Lin, Z. Chen, Z. Quan, Z. Tang, Multiple cellular origins and molecular evolution of intrahepatic cholangiocarcinoma, Cancer Lett. 379 (2) (2016) 253–261.
[49] J. Wu, A.T. Mayer, R. Li, Integrated imaging and molecular analysis to decipher tumor microenvironment in the era of immunotherapy, Semin. Cancer Biol. 84 (2022) 310–328.
[50] M. Porcu, C. Solinas, L. Mannelli, G. Micheletti, M. Lambertini, K. Willard-Gallo, E. Neri, A.E. Flanders, L. Saba, Radiomics and "radi-…omics" in cancer immunotherapy: a guide for clinicians, Crit. Rev. Oncol. Hematol. 154 (2020), 103068.
[51] W.L. Bi, A. Hosny, M.B. Schabath, M.L. Giger, N.J. Birkbak, A. Mehrtash, T. Allison, O. Arnaout, C. Abbosh, I.F. Dunn, et al., Artificial intelligence in cancer imaging: clinical challenges and applications, CA A Cancer J. Clin. 69 (2) (2019) 127–157.
[52] A. Hagiwara, S. Fujita, R. Kurokawa, C. Andica, K. Kamagata, S. Aoki, Multiparametric MRI: from simultaneous rapid acquisition methods and analysis techniques using scoring, machine learning, radiomics, and deep learning to the generation of novel metrics, Invest. Radiol. 58 (8) (2023) 548–560.
[53] M.R. Tomaszewski, R.J. Gillies, The biological meaning of radiomic features, Radiology 298 (3) (2021) 505–516.
[54] Q. Sun, Y. Chen, C. Liang, Y. Zhao, X. Lv, Y. Zou, K. Yan, H. Zheng, D. Liang, Z.-C. Li, Biologic pathways underlying prognostic radiomics phenotypes from paired MRI and RNA sequencing in glioblastoma, Radiology 301 (3) (2021) 654–663.
[55] D. Udayakumar, Z. Zhang, Y. Xi, D.K. Dwivedi, M. Fulkerson, S. Haldeman, T. McKenzie, Q. Yousuf, A. Joyce, A. Hajibeigi, et al., Deciphering intratumoral molecular heterogeneity in clear cell renal cell carcinoma with a radiogenomics platform, Clin. Cancer Res. : Off. J. Am. Assoc. Cancer Res. 27 (17) (2021) 4794–4806.
[56] Y. Zhang, C. Jiang, Postoperative cancer treatments: in-situ delivery system designed on demand, J. Contr. Release 330 (2021) 554–564.
[57] L. Xiang, S. Jin, P. Zheng, E.P. Maswikiti, Y. Yu, L. Gao, J. Zhang, Y. Zhang, H. Chen, Risk assessment and preventive treatment for peritoneal recurrence following radical resection for gastric cancer, Front. Oncol. 11 (2021), 778152.
[58] S. Buettner, B. Koerkamp, A. Ejaz, F. Buisman, Y. Kim, G. Margonis, S. Alexandrescu, H. Marques, J. Lamelas, L. Aldrighetti, et al., The effect of preoperative chemotherapy treatment in surgically treated intrahepatic cholangiocarcinoma patients-A multi-institutional analysis, J. Surg. Oncol. 115 (3) (2017) 312–318.
[59] R.T. Shroff, E.B. Kennedy, M. Bachini, T. Bekaii-Saab, C. Crane, J. Edeline, A. El-Khoueiry, M. Feng, M.H.G. Katz, J. Primrose, et al., Adjuvant therapy for resected biliary tract cancer: ASCO clinical practice guideline, J. Clin. Oncol. : Off. J. Am. Soc. Clin. Oncol. 37 (12) (2019) 1015–1027.
[60] G. Kendre, K. Murugesan, T. Brummer, O. Segatto, A. Saborowski, A. Vogel, Charting co-mutation patterns associated with actionable drivers in intrahepatic cholangiocarcinoma, J. Hepatol. 78 (3) (2023) 614–626.
[61] M. Queiroz, N. Lima, T. Biachi de Castria, Immunotherapy and targeted therapy for advanced biliary tract cancer: adding new flavors to the pizza, Cancers 15 (7) (2023).